# Electronic Supplementary Information (ESI)

# Promotional effects of $In(PO_3)_3$ on the high catalytic activity of CuO-$In(PO_3)_3$/C for $CO_2$ reduction reaction

Chengtao Ruan[a], Zhihui Zhao[a], Hui Wu[a], Jiaqian Liu[a], Yuande Shi[a,b*], Lingxing Zeng[a,c*]and Zhongshui Li[a, b, d*]

[a] *College of Chemistry & Materials Science, Fujian Normal University, Fuzhou 350007, China. E-mail: zsli@fjnu.edu.cn; zenglingxing@fjnu.edu.cn; yuandeshi@fpnu.edu.cn*

[b] *Fujian Province-Indonesia Marine Food Joint Research and Development Center Fuqing 350300, China.*

[c] *College of Environmental and Resource Sciences, Fujian Key Laboratory of Pollution Control & Resource Reuse, Fujian Normal University, Fuzhou 350007, China.*

[d] *Fujian Provincial Key Laboratory of Advanced Materials Oriented Chemical Engineering, Fuzhou 350007, China.*

**E-mail: zsli@fjnu.edu.cn; zenglingxing@fjnu.edu.cn; yuandeshi@fpnu.edu.cn*

## Experimental

### Materials

$C_2H_5OH$ (≥ 99.7%), $KHCO_3$ (≥ 99.5%), $Cu(NO_3)_2 \cdot 3H_2O$ (≥ 99.0%), $In(NO_3)_3 \cdot 3H_2O$ (≥ 99.99%), $PPh_3$ (≥99.5%), NaOH (≥ 99.0%), $Na_2HPO_3$ (≥ 98.0%), $NaH_2PO_2$ (≥ 99.0%) and $NaH_2PO_4$ (≥ 99.0%) were all analytical reagents and purchased from Sinopharm Chemical Reagent Co. Ltd. (Shanghai, China). $D_2O$ (99.9%), HCOOH (> 99%) and $C_2H_6OS$ (≥ 99.95%) were purchased from Aladdin Co. Ltd. (Shanghai, China). Nafion 117 solution (5%) was purchased from Sigma-Aldrish Co. Inc. (USA). The water used in all experiments was purified to a resistivity of 18.25 MΩ cm and deoxygenated with high purity nitrogen before use.

### Characterization methods

X'pert Pro X-ray diffractometer (PANalytical, NED) was employed to record X-ray diffraction (XRD) patterns using Cu Kα radiation between 5° and 90° 2θ at 40 kV and 40 mA. X-ray photoelectron spectroscopy (XPS) was conducted on ESCALAB Xi+ electron spectrometer (Thermo Fisher Scientific, USA) using Al Kα radiation to investigate the surface valance states of samples. Specifically，the spectra were excited using with an Al-Kα radiation source (1486.6 eV) and binding energy was referenced to C1s peak at 284.8 eV. The software "XPSPEAK (Version 4)" was used to treat curve fitting based on a non-linear least-square regression method and linear type background corrections. The morphologies of catalysts were observed by high-resolution transmission electron microscopy (HRTEM), high angle annular dark field-scanning transmission electron microscopy (HAADF-STEM) and the element mappings, which were conducted on TECNAI G2 transmission electron microscope (TEM, FEI, USA). It was also analyzed by scanning electron microscopy (SEM, Zeiss Sigma 500, Germany) to intuitively observe the surface morphology of as-electrodeposited Cu/Ag particles.

### Electrochemical test details

All electrochemical experiments were performed in an electrochemical workstation (CHI 650E, Shanghai, China, three-electrode setup). Electrochemical carbon dioxide reduction ($CO_2$RR) experiments were performed in an H-type electrolytic cell separated by a Nafion N117 membrane, with the anode and cathode chambers filled with 10 ml of 0.5 M $KHCO_3$ solution, respectively. CuO-$In(PO_3)_3$/C, CuO-$In(OH)_3$/C, CuO/C, $In(PO_3)_3$/C coated electrode was used as the working electrode. The auxiliary electrode and the reference electrode were silver chloride electrode (Ag/AgCl) and platinum column electrode, respectively. RHE was used as the reference potential and its value was converted from the Ag/AgCl reference electrode with the equation: E (vs. RHE) = E (vs. Ag/ AgCl) + 0.210 V + 0.0591 V x pH[1, 2]. Linear scanning voltammetry (LSV), constant potential electrolysis (i-t) experiments, electrochemical active surface area testing (ECSA) and electrochemical impedance spectroscopy (EIS), etc. were used to analyze the electrochemical performance of the catalysts. Before electrochemical experiments, oxygen was removed from the H-type electrolytic cell (cathode chamber) and electrolyte by continuously bubbling $N_2$ (99.99%) or $CO_2$ (99.99%) for 30 minutes. Linear scanning voltammetry (LSV) tests were performed in $N_2$ or $CO_2$ saturated 0.5 mol·$L^{-1}$ $KHCO_3$ solution with a potential range from -0.086 V to -1.185 V at 0.01 v $s^{-1}$. The potential of the constant potential electrolysis (i-t) was specified by the LSV curves. The flow rate of $CO_2$ during electrolysis was 20 mL·$min^{-1}$. Electrochemically active surface area (ECSA) of the catalysts was determined in 0.5 M $KHCO_3$ solution using the double-layer capacitance (Cdl) method, starting with a series of cyclic voltammetry tests at different scan rates (20, 30, 40, 50, 60, 70, 80 and 90 mV $s^{-1}$). Especially, a non-Faraday potential range interval (0.414 V vs RHE to 0.614 V

vs RHE) was selected to calculate (Cdl). According to the formula: ECSA = Rf × S = Cdl × $Z^{3, 4}$, Rf, S and Z represent the roughness factor, the actual electrode area involved in the reaction and the constant, respectively, so the value of ESCA can be judged according to the Cdl value. Electrochemical impedance test (EIS) was performed in 0.5 M $KHCO_3$ solution to further investigate the charge transfer kinetic process in the electrocatalytic $CO_2$ reduction, and Nyquist curves were obtained by applying different potentials, in which the semicircle diameter represents the charge transfer resistance (Rct). The current density (Ja) was normalized from the area of the working electrode (1x1 $cm^2$). All experiments were carried out at atmospheric pressure and room temperature (25°C).

Electrochemical experiments performed in flow cell were a four-partself-made microflow cell, and the electrocatalytic reduction of $CO_2$ was investigated for 20 min at each applied potential using a controlled potential electrolysis method. Before electrolysis, the $CO_2$ gas and electrolyte were circulated for 30 min to achieve gas−liquid equilibrium. Catalyst-supported GDE, Ag/AgCl (saturated KCl) electrode equipped with a salt bridge, and squashed nickel foam (0.2 mm thickness, 400 mesh) were used as cathode (for $CO_2$ reduction reaction), are refence electrode, and anode (for $O_2$ evolution reaction), and an anionic exchange membrane was interposed between the cathode and anode chamber. The effective area of GDE was controlled to 1 $cm^2$ (2.0 × 0.5 cm) when assembling the cell, and the silicone gaskets were placed between each chamber for sealing. A total of 250 mL of KOH solution was circulated in a cathode chamber through a peristaltic pump at a constant flow 3.0 $mL \cdot min^{-1}$. Anolyte was circulated through a specially made gas−liquid mixed flow pump instead of the conventional peristaltic pump, which can effectively remove $O_2$ produced in an anode chamber in time. High purity $CO_2$ was purged in the gas chamber through a digital mass flow controller, and the outlet of the gas chamber was connected to the GC system.

**Reduction products measurements**

The gas products produced from electrocatalytic reduction of $CO_2$ were quantitatively analyzed online by gas chromatography (GC, FL9790П, Fuli Analytical Instruments Co., Ltd, China). Flame ionization detector (FID) was used to detect the products such as CO, $CH_4$ and $C_2H_4$, and thermal conductivity detector (TCD) was used to detect $H_2$. The liquid product was analyzed by nuclear magnetic resonance spectroscopy (NMR, Buker 400MHz, Brook Company, Switzerland). The specific operation is as follows: 0.5 mL cathode electrolyte was mixed with 0.1 mL $D_2O$ and 5 uL dimethyl sulfoxide (DMSO) solution, in which DMSO was used as internal standard for qualitative analysis and quantitative calculation. The Faradaic efficiency (FE) calculation formula is as follows: FE=z n F / Q ×100%. Among them, z is the number of electrons transferred, and the number of electrons transferred to generate HCOOH, CO and $H_2$ are all 2; n denotes the number of moles of the specific product, obtained by GC or NMR quantitative analysis; F is the Faradaic constant (96485 C $mol^{-1}$); Q is the total charge (C) consumed by the electrolysis process.

## Supplementary Figures and Tables

**Table S1 The addition amount of precursors for different samples**

| Sample | $Cu(NO_3)_2 \cdot 3H_2O$ | $In(NO_3)_3 \cdot 4H_2O$ | $NaH_2PO_2$ | Carbon Black |
|---|---|---|---|---|
| CuO-$In(PO_3)_3$/C | 0.5 mM | 0.05 mM | 200 mg | 30 mg |
| CuO-$In(OH)_3$/C | 0.5 mM | 0.05 mM | - | 30 mg |
| CuO/C | 0.5 mM | - | 200 mg | 30 mg |
| $In(PO_3)_3$/C | - | 0.05 mM | 200 mg | 30 mg |

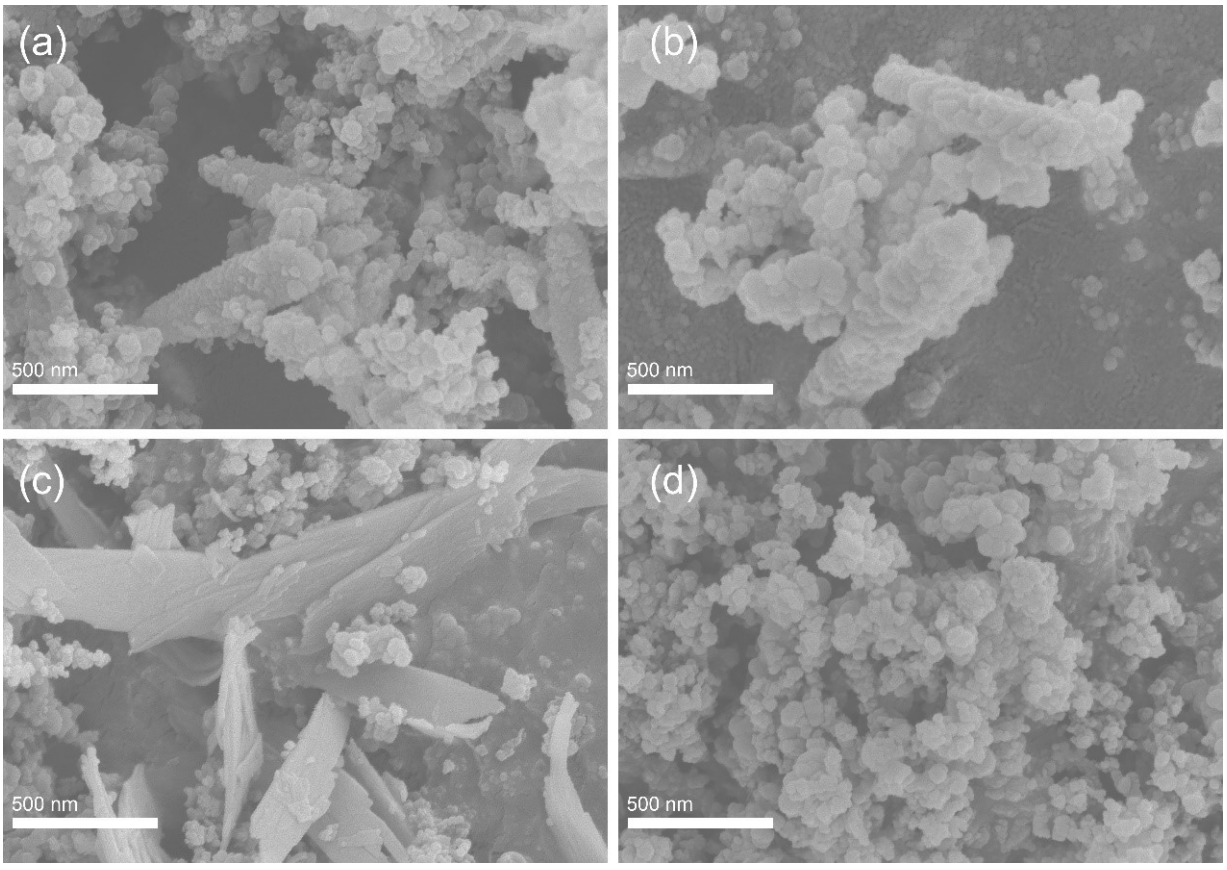


**Fig. S1** SEM images: (a) CuO-$In(PO_3)_3$/C, (b) CuO-$In(OH)_3$/C, (c) CuO/C, (d) $In(PO_3)_3$/C.

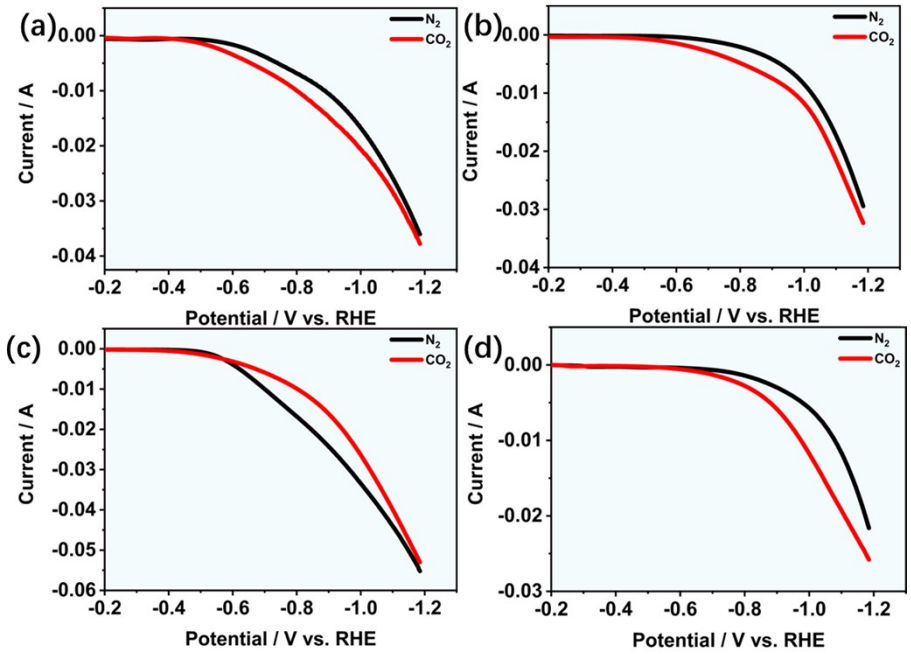


**Fig. S2** Linear sweep voltammetry (LSV) curves in 0.5 M $KHCO_3$ solution saturated with $CO_2$ or $N_2$: (a) CuO-$In(PO_3)_3$/C, (b) CuO-$In(OH)_3$/C, (c) CuO/C, (d) $In(PO_3)_3$/C.

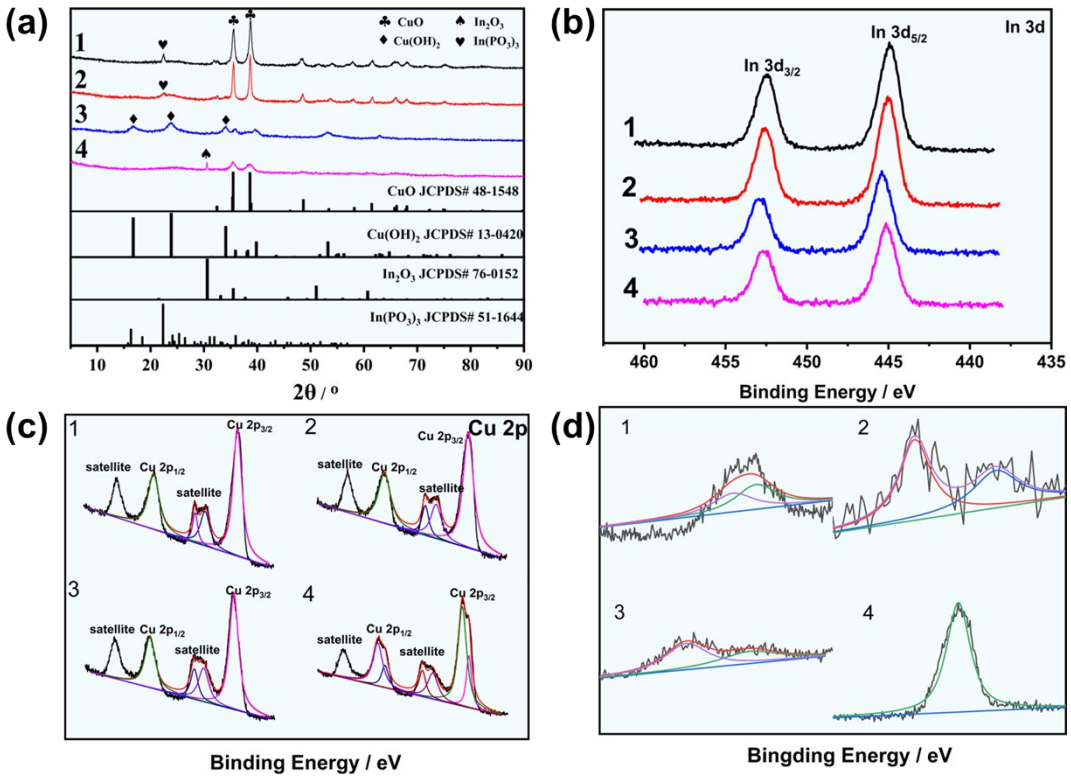


**Fig. S3** Catalysts synthesized with different phosphorus sources: (a) XRD patterns: (1) $PPh_3$, (2) $NaH_2PO_2$, (3) $Na_2HPO_3$, (4) $NaH_2PO_4$; (b) In 3d XPS spectra: (1) $PPh_3$, (2) $NaH_2PO_2$, (3) $Na_2HPO_3$, (4) $NaH_2PO_4$; (c) Cu 2p XPS spectra: (1) $PPh_3$, (2) $NaH_2PO_2$, (3) $Na_2HPO_3$, (4) $NaH_2PO_4$; (d) P 2p XPS spectra: (1) $PPh_3$, (2) $NaH_2PO_2$, (3) $Na_2HPO_3$, (4) $NaH_2PO_4$.

**Table S2 $FE_{CO}$ at -0.586V of catalysts synthesized with different phosphorus sources**

| Cu precursor | P precursors | Main components in as-synthesized catalysts | $FE_{CO}$ / % |
|---|---|---|---|
| $Cu(NO_3)_2$ | $PPH_3$ | CuO, $In(PO_3)_3$ | 6.03 |
| $Cu(NO_3)_2$ | $NaH_2PO_2$ | CuO, $In(PO_3)_3$ | 88.50 |
| $Cu(NO_3)_2$ | $Na_2HPO_3$ | $Cu(OH)_3$, $In(OH)_3$ | 67.81 |
| $Cu(NO_3)_2$ | $NaH_2PO_4$ | CuO, $In_2O_3$ | 72.15 |

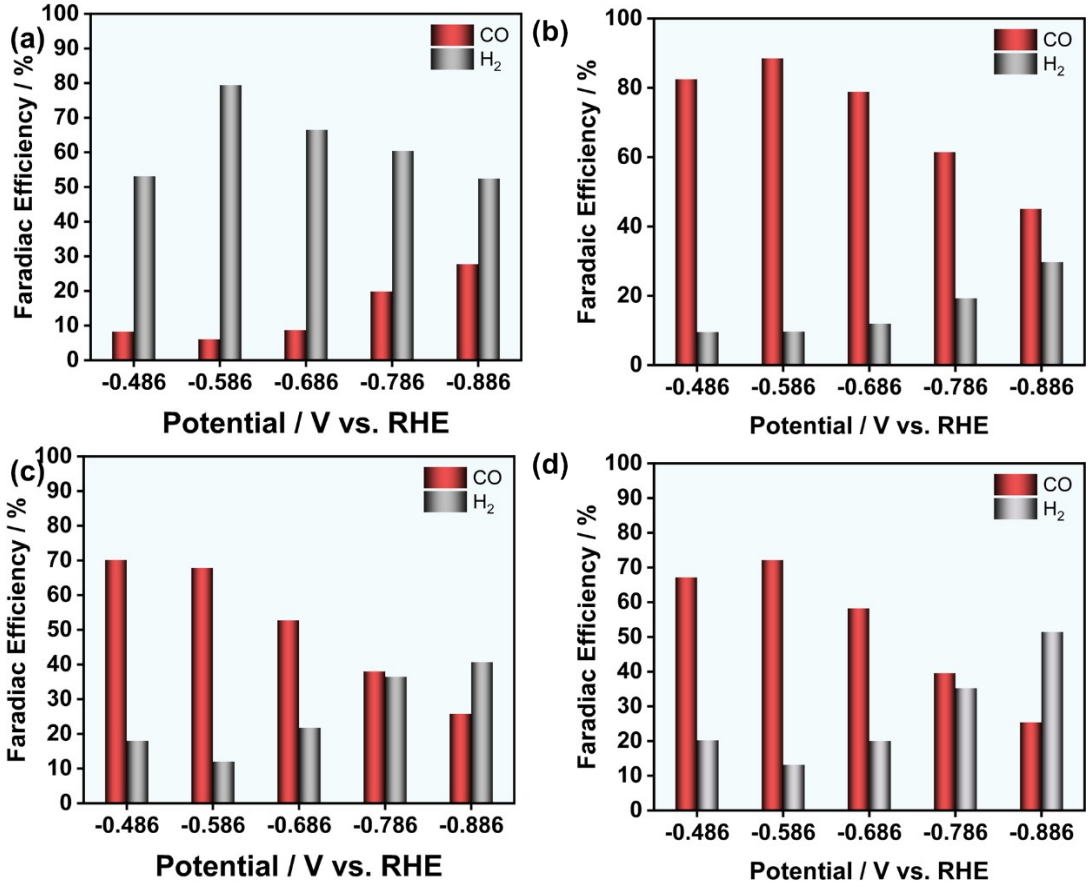


**Fig. S4** Faraday efficiency at different potentials of catalysts synthesized with different phosphorus precursors, in 0.5 M $KHCO_3$ solution saturated with $CO_2$: (a) $PPh_3$, (b) $NaH_2PO_2$, (c) $Na_2HPO_3$, (d) $NaH_2PO_4$

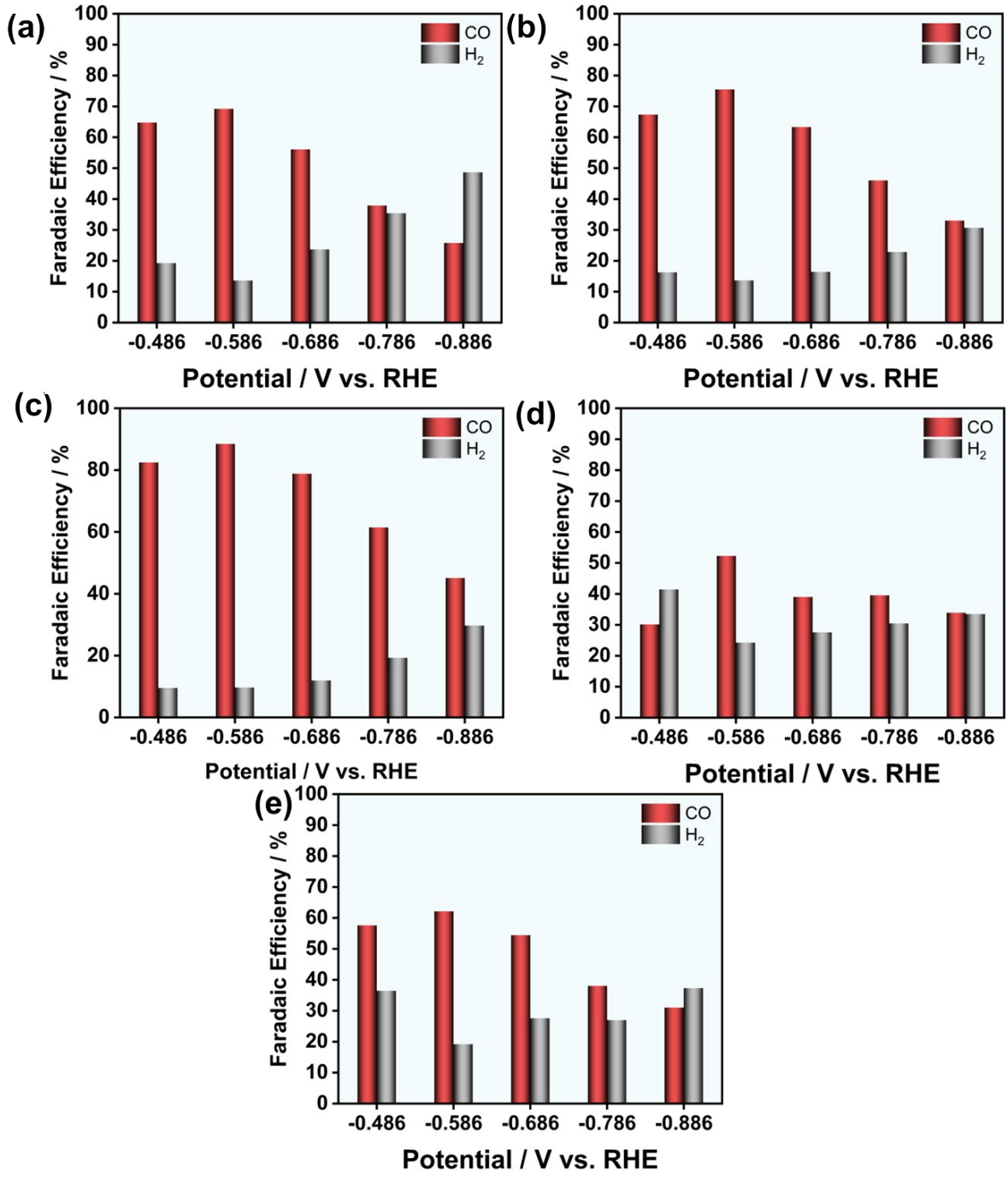


**Fig. S5** Faraday efficiency at different potentials of catalysts synthesized by adding different mass of $NaH_2PO_2$ in 0.5 M $KHCO_3$ solution saturated with $CO_2$: (a) 100mg, (b) 150mg, (c) 200mg, (d) 300mg, (e) 400mg.

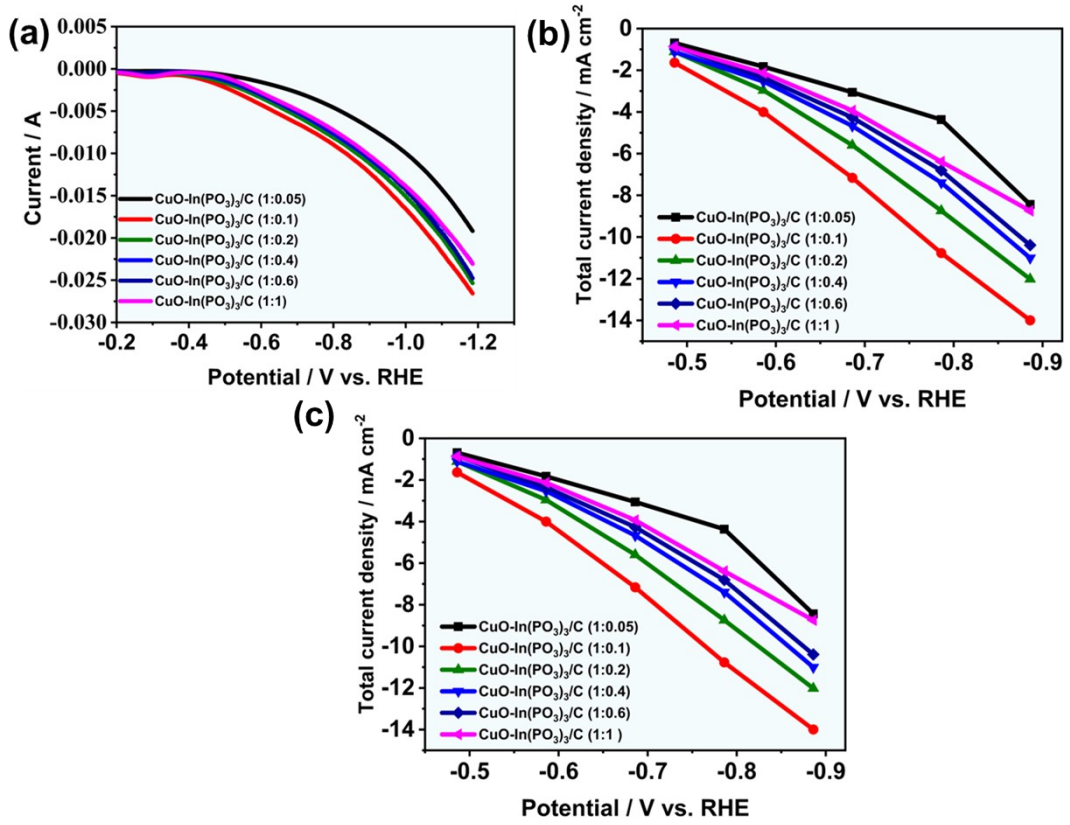


**Fig. S6** (a) LSV curve of catalysts with different ratios of Cu : In in 0.5 M $KHCO_3$ solution saturated with $CO_2$; (b) Total current density; (c) Partial current density.

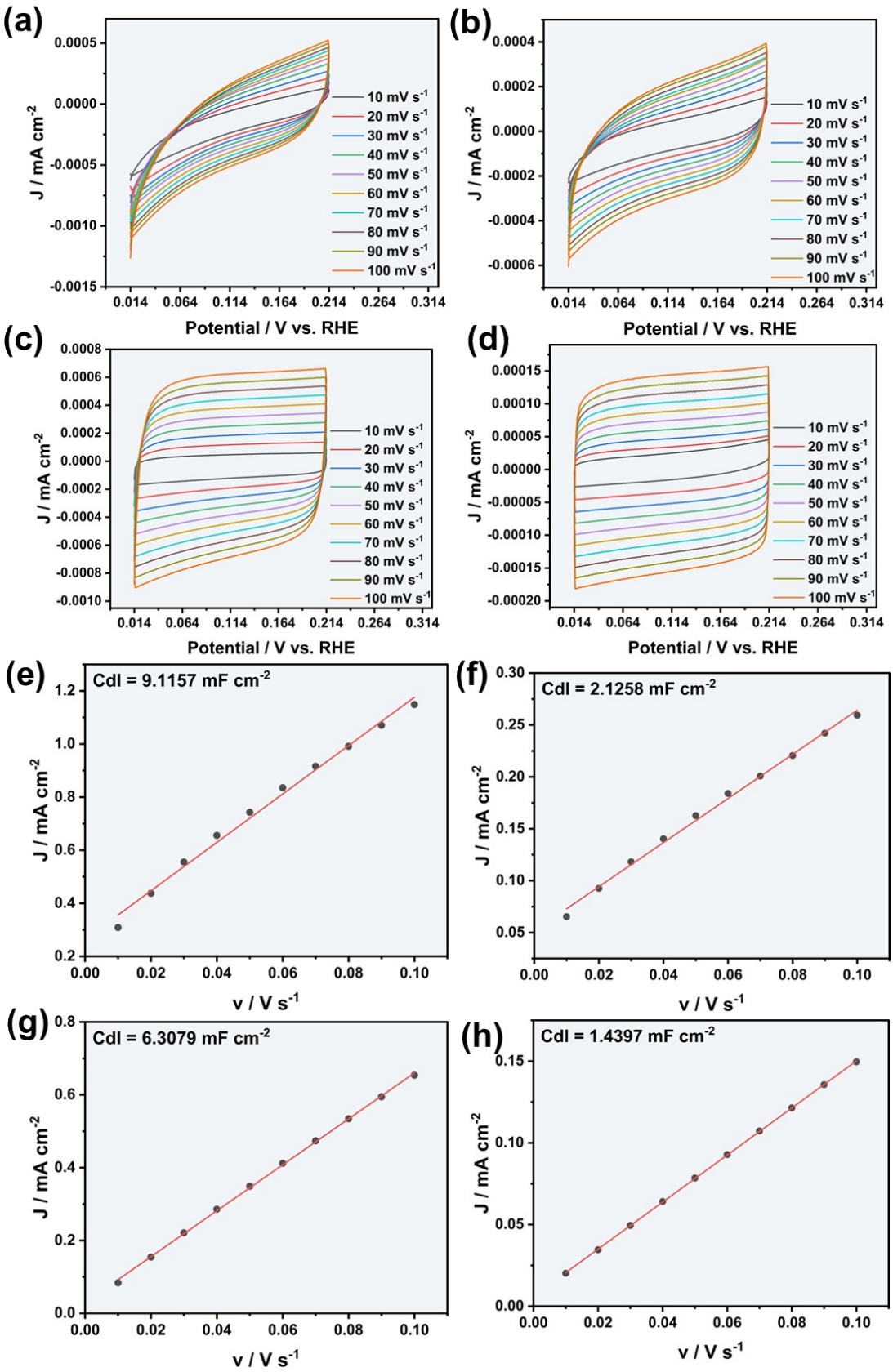


**Fig. S7** CV curves in 0.5 M $KHCO_3$ solution saturated with $CO_2$ at different scanning rate: (a) CuO-$In(PO_3)_3$/C, (b) CuO-$In(OH)_3$/C, (c) CuO/C and (d) $In(PO_3)_3$/C; The calculation curves for ECSA from CV curves **:** (e) CuO-$In(PO_3)_3$/C, (f) CuO-$In(OH)_3$/C, (g) CuO/C and (h) $In(PO_3)_3$/C.

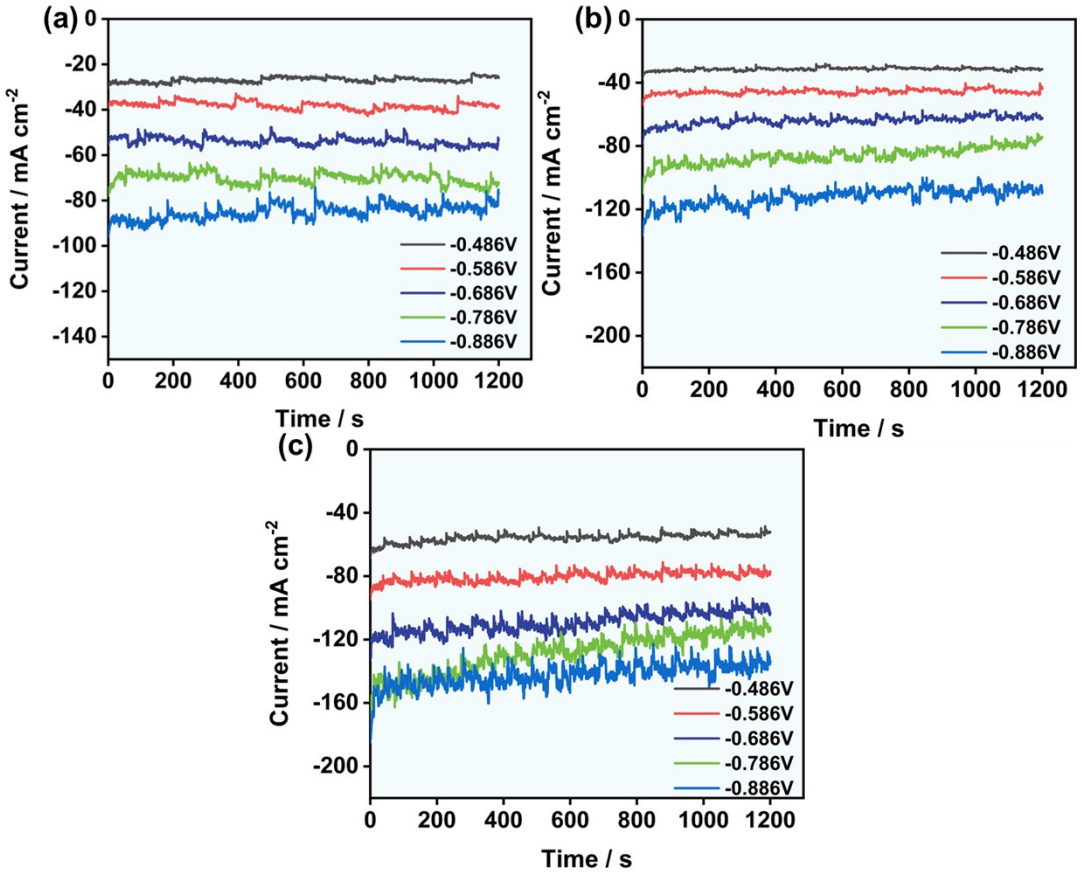


**Fig. S8** Chronoamperometry tests of CuO-In$(PO_3)_3$/C at different electrolyte in Flow Cell: (a) 0.5 M KOH, (b) 1.0 M KOH, (c) 2.0 M KOH.

## References

1 H. Zhang, X. Chang, J. G. Chen, W. A. Goddard, III, B. Xu, M.-J. Cheng and Q. Lu, *Nat. Commun.*, 2019, **10**.
2 B. Qin, Y. Li, H. Wang, G. Yang, Y. Cao, H. Yu, Q. Zhang, H. Liang and F. Peng, *Nano Energy*, 2019, **60**, 43-51.
3 Y. Ye, Y. Liu, Z. Li, X. Zou, H. Wu and S. Lin, *J. Colloid Interf. Sci.*, 2021, **586**, 528-537.
4 J. Gao, H. Zhang, X. Guo, J. Luo, S. M. Zakeeruddin, D. Ren and M. Gratzel, *J. Am. Chem. Soc.*, 2019, **141**, 18704-18714.